Journal of Computer-Aided Molecular Design, **12:** 425–440, 1998.
KLUWER/ESCOM

Aspects of the mechanism of catalysis of glucose oxidase: A docking, molecular mechanics and quantum chemical study

Michael Meyer[a,*], Gerd Wohlfahrt[b,**], Jörg Knäblein[c,***] & Dietmar Schomburg[c,****]
[a]*Institut für Molekulare Biotechnologie (IMB), Biocomputing, Beutenbergstrasse 11, D-07745 Jena, Germany;* [b]*Gesellschaft für Biotechnologische Forschung (GBF), Abt. Enzymologie and* [c]*Molekulare Strukturforschung, Mascheroder Weg 1, D-38124 Braunschweig, Germany*

Received 12 November 1997; Accepted 12 February 1998

Key words: enzyme mechanism, flavoenzyme, force field, ligand docking, QM/MM, semiempirical calculation

Summary

The complex structure of glucose oxidase (GOX) with the substrate glucose was determined using a docking algorithm and subsequent molecular dynamics simulations. Semiempirical quantum chemical calculations were used to investigate the role of the enzyme and FAD co-enzyme in the catalytic oxidation of glucose. On the basis of a small active site model, substrate binding residues were determined and heats of formation were computed for the enzyme substrate complex and different potential products of the reductive half reaction. The influence of the protein environment on the active site model was estimated with a point charge model using a mixed QM/MM method. Solvent effects were estimated with a continuum model. Possible modes of action are presented in relation to experimental data and discussed with respect to related enzymes. The calculations indicate that the redox reaction of GOX differs from the corresponding reaction of free flavins as a consequence of the protein environment. One of the active site histidines is involved in substrate binding and stabilization of potential intermediates, whereas the second histidine is a proton acceptor. The former one, being conserved in a series of oxidoreductases, is also involved in the stabilization of a C4a-hydroperoxy dihydroflavin in the course of the oxidative half reaction.

Introduction

Glucose oxidase (GOX) has found a variety of applications, especially as a biosensor for the quantitative determination of β-D-glucose in liquids. The homodimer is a flavoprotein, which catalyses the oxidation of β-D-glucose in a highly specific way. Other monosaccharides are oxidized at much lower rates. The enzymatic reaction can be divided into two steps. In the first reaction step, two protons and electrons are transferred from β-D-glucose to the enzyme. This reductive half reaction of the catalytic cycle leads to the oxidation of β-D-glucose to δ-gluconolactone as shown in Figure 1. In the second step (the oxidative half reaction) the enzyme is oxidized by molecular oxygen yielding hydrogen peroxide. Finally, δ-gluconolactone can be hydrolysed non-enzymatically to gluconic acid. This hydrolysis has been investigated already with semiempirical quantum chemical calculations [1]. Electron paramagnetic resonance and kinetic studies of the glucose oxidation have been carried out in a pH range between 3 and 10 by Weibel and Bright [2]. They proposed a pH-dependent mechanism, since it is known that the isoalloxazine nucleus of the FAD can be deprotonated at high pH depending on the redox state [3]. The details of the mechanism remained unresolved because no structural information of GOX was available. Our study reveals new aspects of the interactions between glucose, FAD and the active site residues. Additionally, we investigated the stabilization of the C4a-hydroperoxy dihydroflavin

*To whom correspondence should be addressed.
**Present address: VTT Biotechnology and Food Research, Biologinkuja 1, Espoo, P.O. Box 1500, FIN-02044 VTT, Finland.
***Present address: Max-Planck-Institut für Biochemie, Abt. Strukturforschung, Am Klopferspitz 18a, D-82152 Martinsried, Germany.
****Present address: Universität zu Köln, Institut für Biochemie, Zülpicher Strasse 4, D-50674 Köln, Germany.

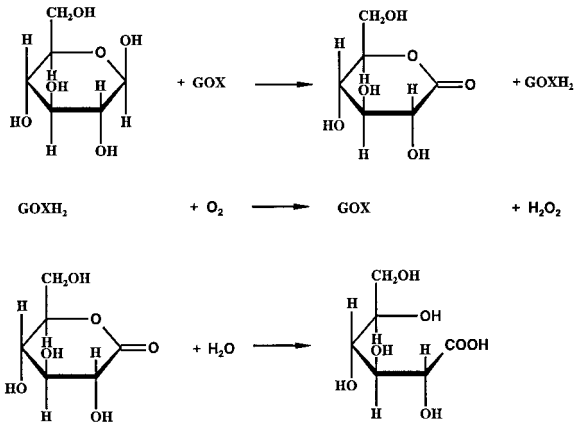

Figure 1. The enzymatic reaction catalysed by glucose oxidase.

by the enzyme environment, which might be a general feature of the flavoenzymes called GMC oxidases [4].

Recently, several studies of model systems for active sites of enzymes have been performed to obtain new insights into catalytic mechanisms. These MO studies have been carried out at semiempirical level [5–17] or at ab initio level [8,10,18–21]. The choice of the method depends mainly on the size of the model system. Often the calculations refer to the gas phase and an influence of the environment has been completely neglected. But the environment can be incorporated into the calculations at different levels [22]. On the one hand, continuum solvent models have been applied [8,19] to estimate the influence of water. Sometimes an effective dielectric has been used to model the combined protein and water influence in an unspecific way [9,10]. On the other hand, specific interactions of the model system with a truncated part of the enzyme have been taken into account. For example, effective fragment potentials have been used to model electrostatic interactions between the chemically active system investigated by ab initio methods and a part of the enzyme environment [18,21].

We carried out computational studies on the basis of the X-ray structure to derive information about the role of the enzyme and its co-enzyme FAD in the catalytic process. The calculations focus on the enzyme substrate complex and on potential products of the reductive half reaction. Additionally, some conclusions can be drawn for intermediates of the oxidative half reaction. Neither the enzyme substrate complex structure nor the structure of the enzyme with a substrate analogous inhibitor is available today. Therefore, we carried out first rigid body docking simulations to find sterically acceptable orientations of β-D-glucose at the active site. Then force field calculations were performed to determine the energetically most favourable orientation. Subsequently, we constructed a small quantum model representing the essential features of the active site with the substrate and investigated it with a mixed QM/MM approach to get an insight into the catalytic mechanism. Charges were computed for the immediate active site environment residues to construct a point charge model (PCM). Finally, the quantum region was investigated at semiempirical level, taking into account electrostatic and van der Waals interactions with this classical environment. For comparison, single point calculations without the PCM environment were carried out to estimate the influence of the ordered protein structure and continuum solvent calculations were performed to determine the effects of an unspecific solvent influence. Mulholland et al. [22] proposed to use model studies in conjunction with experimental results to test the computed results and explain the mechanism. We apply this strategy and propose an extended mechanism based on our calculations and previous kinetic and spectroscopic studies.

Materials and methods

Protein structure

The X-ray structure coordinates of *Aspergillus niger* GOX (PDB entry 1GAL), refined to 2.3 Å resolution by Hecht et al. [23], were used in the initial stage of the study. The final results of the force field and MO calculations were derived from a more recent 1.9 Å structure crystallized at a different pH. Both structures are very similar at the active site region, but two important differences relevant to our study exist. The imidazole ring of His^{516}, a potential proton acceptor in the reductive half reaction (see below), is rotated in a different way in both structures. Furthermore, the side chains of the residues Asp^{424} and Arg^{512}, being potentially involved in substrate binding, have different conformations in both structures. The latter residues are part of the fixed protein environment in our semiempirical calculations. Therefore, the rigid body docking simulations and the semiempirical calculations were carried out for each conformation.

Docking

Docking simulations with β-D-glucose and δ-gluconolactone were carried out with correlation techniques

[24]. The glucose structure was taken from Chu and Jeffrey [25] in the first docking run. Later the calculations were repeated with the conformation determined from MD simulations described below. Both computed orientations of the ligands were essentially identical. A truncated model of the enzyme with all atoms within a radius of 10 Å about the atom N5 of FAD was used. The active site was represented without explicit hydrogen atoms on a grid with a spacing of 1.2 Å, and an angular step size of 22.5° was selected in the fast initial scan for ligand rotations. The subsequent simplex refinement of the enzyme ligand orientation was carried out at 0.8 Å grid point distance.

Force field calculations

Subsequently to the rigid body docking of glucose into the substrate-binding pocket of GOX described above, a flexible refinement with molecular mechanics methods was carried out to form the non-covalently bonded Michaelis complex. The protein modelling package BRAGI [26] and the molecular mechanics program AMBER 4.0 [27] were used for these simulations and for the analysis of the resulting structures. The AMBER all-atom force field [28] was used with additional parameters for glucose and FAD. These parameters were fitted to reproduce experimental data of these molecules and some smaller model compounds. The glucose parameters are much the same as the corresponding GLYCAM parameters for oligosaccharides [29]. Histidines were assumed to be protonated at both nitrogens in accordance with the overall charge determination of Voet et al. [30] with the exception of the active site histidines whose protonation state was changed in some calculations. Fifteen crystallographic water molecules from the active site region were added to the system and the AMBER EDIT program was used to fill the space within a 10 Å radius of the N5 of isoalloxazine with TIP3P water molecules [31]. The water molecules were constrained to the centre of the sphere by a harmonic potential with a force constant of 0.5 kcal/mol $Å^2$. Only the atoms of the residues inside the 10 Å radius were allowed to move during these simulations. The force field calculations were carried out at a dielectric constant of 1. An 8 Å cut-off distance for non-bonded interactions was used. During the molecular dynamics (MD) simulations, the SHAKE algorithm [32] was used to constrain the covalent bonds to their equilibrium bond length. The structures were energy-minimized and then equilibrated by molecular dynamics for 50 ps at 298 K with an integration interval of 1 fs. The resulting structures were again energy-minimized and analysed for their similarity to the X-ray structure and their energetic and geometric properties.

Ab initio calculations

Atomic charges for the force field calculations were derived from hybrid density functional calculations for flavins, glucose and gluconolactone using an electrostatic potential fitting method [33,34] at the B3LYP/6-31G* level [35–37]. The flavin charges resemble those determined by Peräkala and Pakkanen [38]. Furthermore, structure optimizations were carried out at the B3LYP/6-31G** level with GAUSSIAN 94 [39] and at the MP2/6-31G* level of theory with GAMESS [40] to compare ab initio and semiempirical results for hydrogen bonding between imidazole and acetate. The functionality of these molecules is equivalent to that of histidine and glutamate side chains.

Semiempirical calculations

The semiempirical PM3 method [41] implemented in Vamp 6.1 [42] and AMSOL 5.4 [43] was used throughout. The interaction between the quantum system and the classical enzyme environment was taken into account using a point charge model, which includes an electrostatic perturbation of the quantum system wave function and van der Waals interactions with the environment (T. Clark et al., to be published). The influence of the solvent on the quantum system has been investigated using the PM3-SM3.1 model [44] of AMSOL 5.4.

Quantum region

The number of atoms which can be included in the quantum region representing the active site is limited. Therefore, we restricted this region to FAD and the residues being potentially involved in the redox reaction, i.e. His^{516}, His^{559} and Glu^{412}. For the investigation of the complexes glucose, the oxyanion of glucose and gluconolactone were added to the active site in relative orientations and in conformations corresponding to the results of the docking and MD simulations. Small model molecules were substituted for the active site residues in the same relative orientation as in the GOX structure, because the program cannot handle bonds between the PCM environment and the quantum system. FAD is represented by lumiflavin (Fl = 7,8,10-trimethyl isoalloxazine), methyl

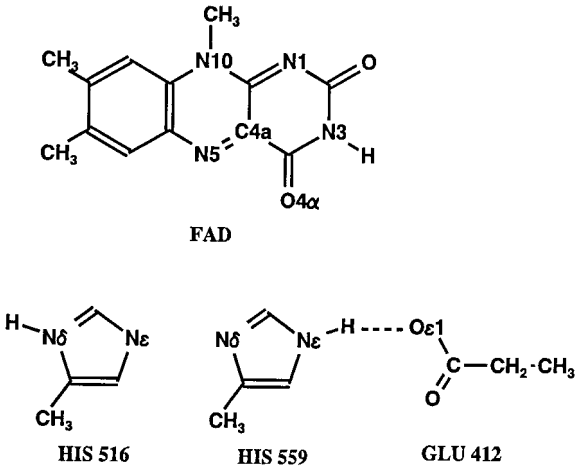

Figure 2. The active site model of GOX. The tautomers correspond to row no. 1 in Table 1.

imidazole (MI516, MI559) is used for His and a propionate ion ($P412^-$) mimics Glu. The functional groups of these model molecules shown in Figure 2 correspond to those of FAD and the active site residues. We keep the numbering of the residues and their individual atoms to indicate the assignment between the model and the enzyme. Weibel and Bright [2] had come to the conclusion that a deprotonation step is necessary at low pH to obtain a catalytically active GOX. We assumed a high pH with unprotonated histidines and an overall quantum system charge of -1 according to Figure 2. There are no further residues close to N5 of the FAD, which can act as proton or electron relay system on the substrate.

To construct a physically meaningful mimic of the enzyme active site, some structural constraints had to be imposed to prevent the movement of parts of the quantum region to unrealistic positions during structure optimization processes. We fixed the Cartesian coordinates of the methyl group carbon atom at N10 of Fl and the MI and $P412^-$ methyl group carbon atoms to relative orientations corresponding to the experimental enzyme structure using default force constants. The latter carbon atoms correspond to the Cβ atoms of His and Glu. Test optimizations without structural constraints in the enzyme environment showed only minor deviations relative to the enzyme structure, except for MI516. The corresponding His^{516} has a high temperature factor in the X-ray structure indicating side chain mobility and both available experimental GOX structures differ in the torsion angles of the His side-chain. The other residues hardly move since they are fixed by hydrogen bonds to the PCM environment. Of course, no structural constraints were opposed for the substrate and product in complexes during optimizations within the classical environment.

Single point calculations were carried out at the optimized quantum system without the environment to determine the protein influence on the active site. Individual residues were excluded from the environment to estimate the influence of these residues on the calculated heats of formation. The PM3-SM3.1 solvent model was applied to determine free energies of solvation (ΔG_s^0) and to get an estimate as to whether or not water might change the order of the relative energies.

Point charge environment

The point charge environment was limited to 53 GOX residues having at least one atom within a radius of 12 Å around FAD N5 and 10 Å around the other quantum active model residues. This environment includes the substrate binding residues and the immediate neighbours of the catalytically active part, which do not participate in a direct way in the chemical reaction. Atomic coordinates were taken directly from the X-ray structures, hydrogen atoms were added using standard geometrical parameters and non-bonded residues were capped at the termini with additional hydrogen atoms. We assumed Asp, Glu, Lys and Arg residues to be charged. The environment was divided first into four groups of unconnected residues since the system is too large for a single charge calculation at the semiempirical level. For each group, atomic charges were computed using the natural atomic orbital/point charge model [45]. In this model, each hydrogen atom is represented by a single point charge and each non-hydrogen atom is represented by the positive core charge and eight negative charges for the electron cloud calculated from natural atomic orbitals and their occupancies. Finally, the groups were combined to give the complete PCM environment used for semiempirical calculations. All in all, an environment of 901 atoms and 4382 point charges was constructed having a fixed relative orientation corresponding to the enzyme structure. To overcome the limiting factor of rigidity somewhat, we used two different fixed orientations for the hydroxy groups of Tyr^{68} since this residue is located close to the substrate in a complex. Furthermore, we used different fixed side-chain structures of Asp^{424} and Arg^{512} corresponding to the experimental conformations. It turned out that the side-chain conformations of the experimental structure with the higher resolution lead to a lower heat of formation for the enzyme substrate complex.

Results

Docking simulations

Docking calculations with glucose indicate that there is only one substrate orientation at the active site corresponding to a high correlation, i.e. a good shape complementarity. This is a substrate orientation at the bottom of the active site funnel with the hydrogen atom H(C1) of the substrate located in the vicinity of FAD N5, the hydride acceptor. The hydroxy group at C1 is directed roughly between His^{516} and His^{559}. Docking simulations with gluconolactone led to a similar relative orientation at the active site.

Force field calculations

Initial force field calculations were then carried out in order to analyse the tautomeric state and orientation of His^{516} in the presence of glucose. In a first step, we generated six different structural data sets with three different protonation states of the nitrogen atoms Nδ and Nϵ of this His and two orientations of its side chain (the ring is rotated 180°) for each tautomer. Furthermore, initial structures with different torsion angles of the exocyclic hydroxy methylene group of β-D-glucose were generated to find the conformer with the lowest energy and to investigate the hydrogen bonds, which may stabilize orientation of the substrate. Then we minimized the energy of all complexes. In order to save computational time and to avoid distortion of the enzyme structure, we fixed the coordinates of all residues lying outside a 10 Å radius around the FAD N5 atom. To look for additional low-energy conformations of glucose at the active site, we carried out MD simulations starting from selected low-energy structures and minimized the energy again. For comparison, all calculations were repeated for α-D-glucose.

The energetically most favourable system that we found was the one with hydrogen atoms at His^{559} Nϵ and at His^{516} Nδ. The carboxy oxygen Oϵ1 of Glu^{412} is located at a distance of 2.8 Å to His^{559} Nϵ which facilitates the formation of a hydrogen bond to H(Nϵ). The structure of these residues is shown in Figure 3 with the best orientation of β-D-glucose. The 1, 3 and 5 hydroxyl groups of β-D-glucose act as hydrogen donor and acceptor at the same time. Therefore, eight classical hydrogen bonds and the C1-H···N5 hydrogen bond stabilize the orientation of β-D-glucose at the active site. In addition to these highly specific hydrogen bonds which are only possible in this orientation of glucose, the hydrophobic parts of glucose are in contact with unpolar surface areas of the protein (Tyr^{68}, Phe^{414}, Trp^{426}). It is also obvious from Figure 4 that there is no space for a different orientation of glucose if the basic assumption is made that the reacting OH and CH groups should be close to the isoalloxazine ring.

The optimized distance between H(C1) of β-D-glucose and N5 of the FAD co-enzyme is 2.4 Å and H(O1) of the substrate is located 1.8 Å away from the unprotonated Nδ of His^{559}. These favourable distances do not exist for the α-anomeric species as a consequence of the interchange of the hydroxy group and the hydrogen at C1. For example, in the α-D-glucose complex the distance between H(O1) and Nδ of His^{559} is extended to 2.0 Å and that between H(C1) and N5 of FAD to 2.7 Å. The α-D-glucose forms only seven intermolecular hydrogen bonds and one intramolecular hydrogen bond with less favourable angles and distances compared to the β-anomer. The number of hydrogen bonds between GOX and 2-deoxy glucose, which is oxidized at a lower rate [46], is smaller.

The analysis of the short distances between FAD and His residues of GOX on the one hand and H(O1) and H(C1) of β-D-glucose on the other hand leads to a hypothesis for the reaction mechanism, which is deduced from the geometry (Figures 2–4). It seems most likely that H(C1) of β-D-glucose is transferred to N5 of FAD, and H(O1) may be transferred to Nδ of His^{559}, which thereby becomes positively charged. Subsequently, the proton at Nϵ of His^{559} may be transferred to the Oϵ1 of Glu^{412}. This potential mechanism of the enzymatic reaction differs from the corresponding two-electron reductions of free flavins with a transfer of the hydrogens to N1 and N5 of the isoalloxazine ring. A proton transfer to N1 of the FAD of GOX is unlikely because N1 is located at the opposite side of the estimated substrate position (Figure 3) and it is surrounded by enzyme residues. Similarly, a proton transfer to Nϵ of His^{516} seems less probable since this His is not activated by a Glu or Asp.

MO calculations for individual model molecules

Detailed test calculations for different semiempirical methods have been reported [47]. In order to get an impression of the performance of the PM3 method for the model molecules, we computed heats of formation (ΔH_f), proton affinities and structures for related molecules before we investigated the protein model. We selected acetic acid and imidazole for the test since

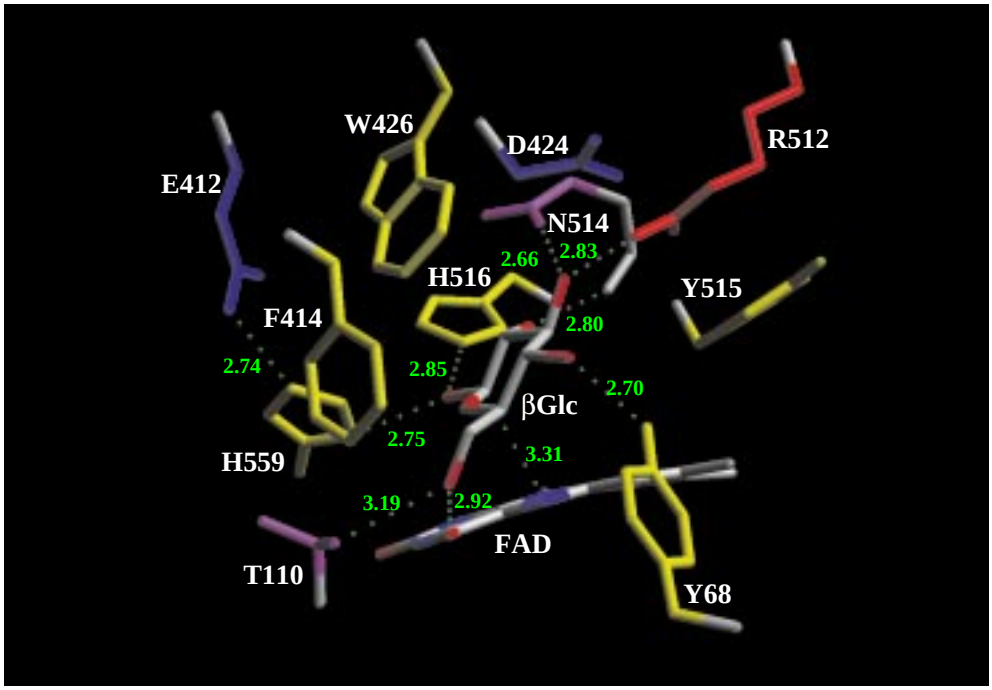

Figure 3. β-D-Glucose at the substrate binding site of GOX. Donor–acceptor atom distances are given; hydrogen atoms have been omitted for clarity.

sufficient experimental and theoretical data are available for these molecules. The results are summarized briefly below.

The calculated ΔH_f of 31.3 kcal/mol [48] is much the same as the experimental result of 31.76 ± 0.1 kcal/mol [49] for imidazole. Proton affinities of imidazole (225.2 kcal/mol) and 4-MI (227.8 kcal/mol) [49] are well reproduced by PM3 (218.3 and 220.9 kcal/mol). There is not much difference between the 4-MI proton affinity and the experimental His proton affinity 236.1 kcal/mol [49]. Similarly, the experimental heats of protonation for acetate and propionate (348.1 and 347.4 kcal/mol) [49] agree well with the PM3 results (348.1 and 347.1 kcal/mol). The calculated proton affinities have been derived from the experimental $\Delta H_f = 365.7$ kcal/mol for H^+ [49] and ΔH_f has been calculated with PM3 for the other species.

There has been much discussion about the interaction of Glu or Asp with a protonated His [50]. A zwitterionic or a neutral complex is conceivable. We carried out optimizations of the model complex imidazolium acetate consisting of ionic species and of the neutral imidazole acetic acid complex. The initial geometries were taken from the experimental GOX structure. PM3 finds a local minimum for the charged complex, but ΔH_f of the neutral complex is 19.8 kcal/mol lower. The corresponding ΔH_f of the transition state is -52.0 kcal/mol and the activation energy is 4.9 kcal/mol. This result is qualitatively the same if other model molecules are used, e.g. formate instead of acetate. Our finding of a local minimum for a charged complex agrees with previous calculations [50] with a different initial geometry corresponding to serine proteases.

The imidazolium acetate and imidazole acetic acid complexes are small enough to be optimized at B3LYP/6-31G** and MP2/6-31G* levels of theory. No transition states were located with both methods and all optimizations converged to the same planar imidazole acetic acid complex structure. The density functional distances r(NH) = 1.735 Å and r(OH) = 1.003 Å are close to the structural parameters of the lower PM3 minimum (r(NH) = 1.78 Å and r(OH) = 0.98 Å). The computed intermolecular distances between the carboxy oxygen atoms and the imidazole

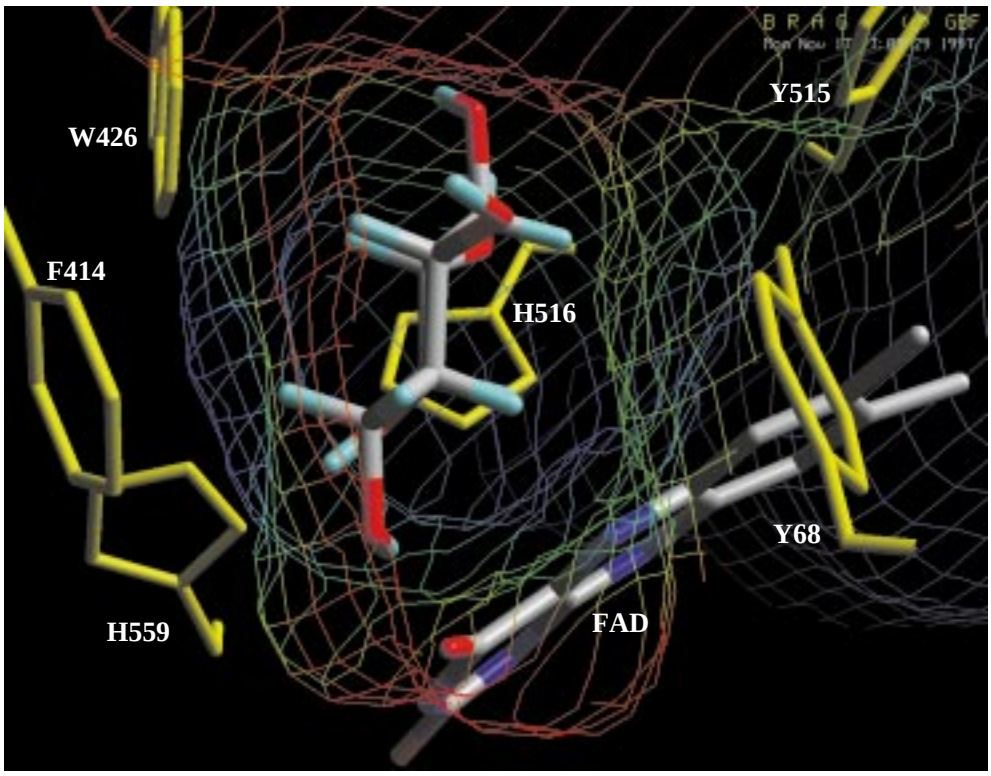

Figure 4. The Connolly surface of the active site of GOX. Enzyme surface colours are from red (polar) over green (neutral) to blue (hydrophobic). The hydrophobic side chains of Tyr^{68}, Phe^{414}, Trp^{430} (in yellow) and a part of the isoalloxazine are in direct contact with unpolar parts of glucose.

nitrogen of the model complex (PM3: 2.75 and 3.36 Å; B3LYP: 2.741 and 3.302 Å) are close to the corresponding distances between His^{559} Nϵ and the oxygen atoms Oϵ1 (2.89 Å) and Oϵ2 (3.28 Å) of Glu^{412} in the experimental protein structure.

Lumiflavin can exist in three different redox states: the oxidized quinone (Fl_{ox}), the one-electron reduced semiquinone, which is not considered in this study, and the two-electron reduced hydroquinone (Fl_{red}). For each of these redox states, cationic, neutral and anionic species exist depending on the number of hydrogen atoms. In principle, different tautomers may exist, too. We give the labels of the nitrogen or oxygen atoms with a bond to a hydrogen atom in parentheses. For example, the oxidized neutral tautomer with hydrogen at N3 is described as $Fl_{ox}H(N3)$ (Figure 5). Detailed semiempirical, ab initio and density functional studies of flavins in different redox states have been carried out [38,51–54]. Semiempirical PM3 calculations predict the same most stable tautomers like ab initio or density functional calculations, except for interchanged relative energies between two tautomeric cations in the oxidized and one-electron reduced state. However, this is only an effect of the neglect of the environment, since the inclusion of a solvation model leads to results consistent with the experiment.

Enzyme substrate and product complexes

The heats of formation for the tautomeric states of the enzyme substrate complex are listed in Table 1. The most stable one (row no. 1, $\Delta H_f = -571$ kcal/mol) has a proton at MI559 Nϵ forming a hydrogen bond with $P412^-$, as indicated in Figure 2. The PM3 optimized position of glucose at the active site is nearly independent of the protonation state and it is close to the structure determined by MD simulations. Hydrogen bonds fixing the substrate are formed between the O4α atom of $Fl_{ox}H(N3)$ and glucose H(O6), Thr^{110} OG1 and O6, Tyr^{68} OH and O4, Asp^{424} Oδ2 and H(O4), Arg^{512} NH1 and O3, Asn^{514} Oδ1 and H(O3). However, the distances between H(C1) and FAD N5 and between H(O1) and MI516 and MI559 are somewhat larger than those determined by the force field calculations. This is probably an effect of the rigid

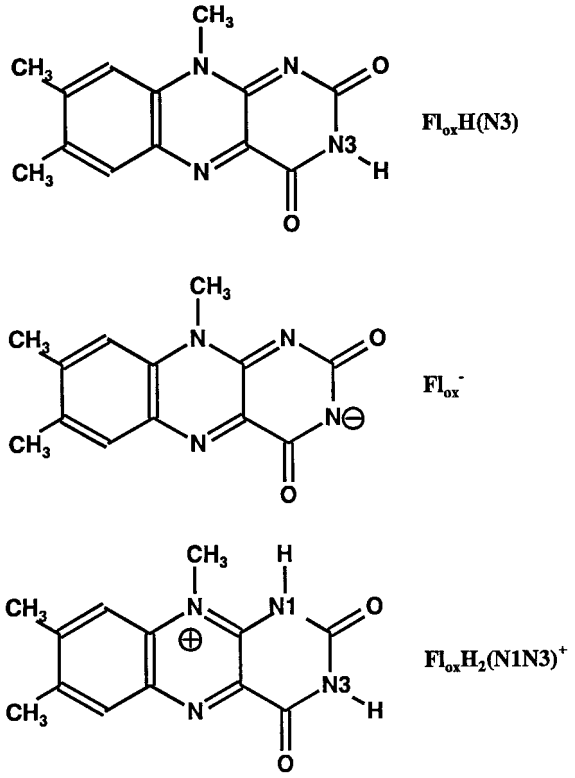

Figure 5. Lumiflavin with protonated and deprotonated derivatives in the oxidized state (*si*-side).

environment which fixes the substrate with hydrogen bonds and prevents a glucose position more closely to the chemically active residues.

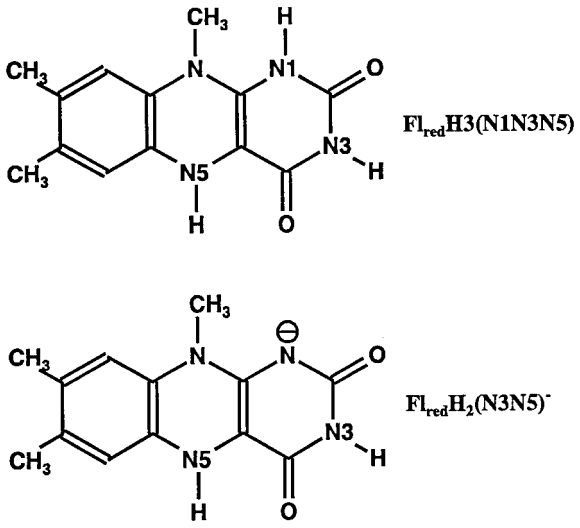

Figure 6. Two-electron reduced derivatives of lumiflavin.

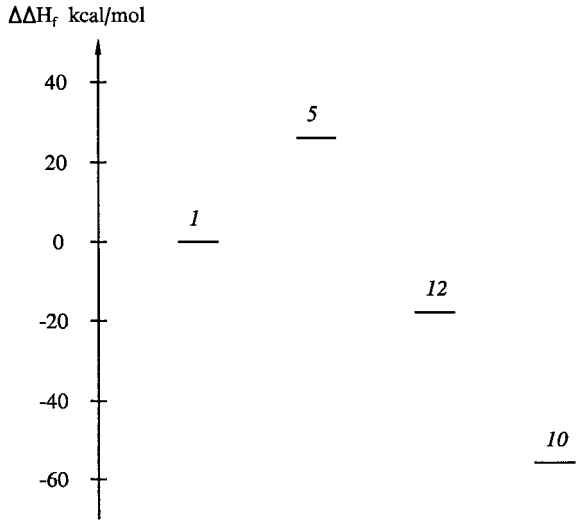

Figure 7. Relative heats of formation for the reductive half reaction (no. 1, enzyme substrate complex; no. 10, enzyme product complex; nos. 5 and 12, potential intermediates, compare Table 1).

For the product of the reductive half reaction, the heats of formation for several tautomers are given in Table 1. The most stable system (no. 10) with $\Delta H_f = -626$ kcal/mol consists of $Fl_{red}H_2^-$(N3N5) (Figure 6), MI516 and MI559 with hydrogen atoms at Nδ and propionic acid with the hydrogen at Oϵ1. The energy difference between the enzyme substrate and product complexes is 55 kcal/mol. The transfer of both hydrogens from glucose to the co-enzyme atoms N1 and N5, which occurs in free flavins, is 37 kcal/mol more unfavourable in the enzyme (no. 14). Gluconolactone does not form a hydrogen bond with $Fl_{red}H_2^-$(N3N5) because this ligand is located somewhat more distant to the co-enzyme than glucose in the enzyme substrate complex.

For some potential intermediates of the enzymatic glucose oxidation, the heats of formation are also listed in Table 1 and the relative heats of formation are shown in Figure 7. If the catalytic oxidation of glucose starts with proton transfer from the glucose hydroxy group -O1H to the enzyme, an oxyanion is formed in the first step (no. 5). This anion can be stabilized by weak hydrogen bonds of 2.0 Å length between the hydrogen atoms Cϵ-H of MI516 and MI559 and the negatively charged oxygen atom O1. A heat of formation of −544 kcal/mol results for this model system with a double protonated MI559 as intermediate. A subsequent hydride transfer from the oxyanion to N5 may decrease ΔH_f to −601 kcal/mol (no. 12), which is 29 kcal/mol lower than the corresponding value for

Table 1. Heats of formation ΔH_f for complexes of the active site model in the protein PCM environment

					ΔH_f (kcal/mol)	$\Delta\Delta H_f$ (kcal/mol)
Oxidized active site model + glucose						
1	$Fl_{ox}H$(N3)	MI559(Nϵ)	P412$^-$	MI516(Nδ)	−571	–
2	$Fl_{ox}H$(N3)	MI559(Nϵ)	P412$^-$	MI516(Nϵ)	−567	4
Oxidized active site model (protonated) + oxyanion of glucose						
3	$Fl_{ox}H$(N3)	MI559(Nδ)	PH412	MI516(Nδ)	−565	–
4	$Fl_{ox}H$(N3)	MI559(Nδ)	PH412	MI516(Nϵ)	−555	10
5	$Fl_{ox}H$(N3)	MI559$^+$(NδNϵ)	P412$^-$	MI516(Nδ)	−544	21
6	$Fl_{ox}H$(N3)	MI559$^+$(NδNϵ)	P412$^-$	MI516(Nϵ)	−536	29
7	$Fl_{ox}H_2{}^+$(N1N3)	MI559(Nϵ)	P412$^-$	MI516(Nδ)	n.s.	
8	$Fl_{ox}H_2{}^+$(N1N3)	MI559(Nϵ)	P412$^-$	MI516(Nϵ)	n.s.	
9	$Fl_{ox}H$(N3)	MI559(Nϵ)	P412$^-$	MI516$^+$(NδNϵ)	−531	34
Reduced active site model + gluconolactone						
10	$Fl_{red}H_2^-$(N3N5)	MI559(Nδ)	PH412	MI516(Nδ)	−626	–
11	$Fl_{red}H_2^-$(N3N5)	MI559(Nδ)	PH412	MI516(Nϵ)	−623	3
12	$Fl_{red}H_2^-$(N3N5)	MI559$^+$(NδNϵ)	P412$^-$	MI516(Nδ)	−601	25
13	$Fl_{red}H_2^-$(N3N5)	MI559$^+$(NδNϵ)	P412$^-$	MI516(Nϵ)	−594	32
14	$Fl_{red}H_3$(N1N3N5)	MI559(Nϵ)	P412$^-$	MI516(Nδ)	−589	37
15	$Fl_{red}H_3$(N1N3N5)	MI559(Nϵ)	P412$^-$	MI516(Nϵ)	−584	42
16	$Fl_{red}H_2^-$(N3N5)	MI559(Nϵ)	P412$^-$	MI516$^+$(NδNϵ)	−597	29
Reduced active site model with oxygen						
17	$Fl_{red}OOH_2^-$(N3N5)	MI559(Nδ)	PH412	MI516(Nδ)	−288	–
18	$Fl_{red}OOH_2^-$(N3N5)	MI559(Nδ)	PH412	MI516(Nϵ)	−288	0
19	$Fl_{red}OOH_2^-$(N3N5)	MI559$^+$(NδNϵ)	P412$^-$	MI516(Nδ)	−262	26
20	$Fl_{red}OOH_2^-$(N3N5)	MI559$^+$(NδNϵ)	P412$^-$	MI516(Nϵ)	−262	26
21	$Fl_{red}OOH_3$(N1N3N5)	MI559(Nϵ)	P412$^-$	MI516(Nδ)	n.s.	
22	$Fl_{red}OOH_3$(N1N3N5)	MI559(Nϵ)	P412$^-$	MI516(Nϵ)	n.s.	
23	$Fl_{red}OOH_2^-$(N3N5)	MI559(Nϵ)	P412$^-$	MI516$^+$(NδNϵ)	−289	−1
Reduced active site model with oxygen (tautomeric flavin)						
24	$Fl_{red}OOH_2^-$(N3O)	MI559(Nδ)	P412$^-$	MI516(Nδ)	−312	−24
25	$Fl_{red}OOH_2^-$(N3O)	MI559(Nδ)	P412$^-$	MI516(Nϵ)	−345	−57
26	$Fl_{red}OOH_2^-$(N3O)	MI559(Nϵ)	P412$^-$	MI516$^+$(NδNϵ)	−313	−25
27	$Fl_{red}OOH_3$(N3N5O)	MI559(Nϵ)	P412$^-$	MI516(Nδ)	−319	−31
28	$Fl_{red}OOH_3$(N3N5O)	MI559(Nϵ)	P412$^-$	MI516(Nϵ)	−313	−25

n.s.: not stable.

the enzyme substrate complex. A final proton transfer of H(Nϵ) from MI559$^+$(NδNϵ) to Oϵ1 of Glu^{412} may lead to the final $\Delta H_f = -626$ kcal/mol (no. 10).

Reduced active site with oxygen

The oxidative half reaction of GOX is a re-oxidation with molecular hydrogen (Figure 1). Two-electron reduced flavins are known to form C4a-hydroperoxy dihydroflavin species with molecular oxygen (Figure 8) [3,53,55]. In Table 1, the heats of formation for such intermediates of the oxidative half reaction are listed. If molecular oxygen reacts with $Fl_{red}H_2^-$(N3N5) to form $Fl_{red}OOH_2^-$(N3N5) and the protonation of other active site residues remains unchanged, a hydrogen bond of 1.68 Å length can be formed between MI559 H(Nδ) and the terminal oxygen of $Fl_{red}OOH_2^-$(N3N5) (Figure 8, top). The corre-

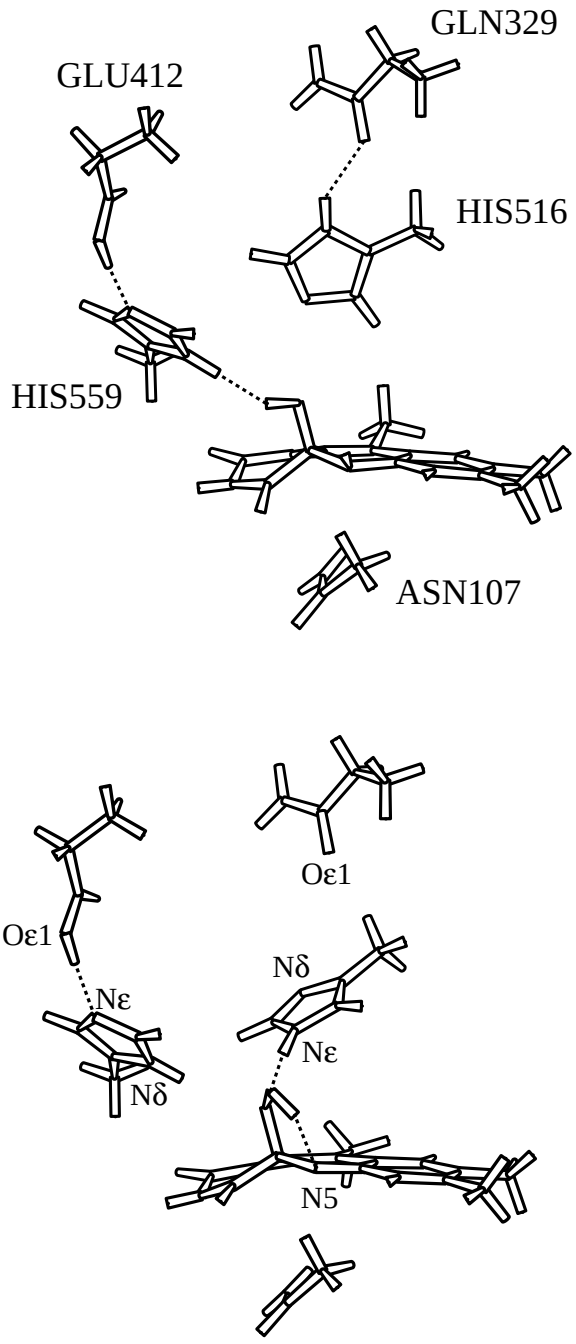

Figure 8. Stabilization of C4a-hydroperoxy dihydrolumiflavin anion and a more stable tautomer with hydrogen bonds at the GOX active site (MOLSCRIPT figure [65]). Top: $Fl_{red}OOH_2^-$(N3N5), MI559(Nδ), PH412, MI516(Nδ), Gln^{329} (compare Table 1, no. 17); Bottom: $Fl_{red}OOH_2^-$(N3O), MI559(Nδ), PH412, MI516(Nϵ), Gln^{329} (Table 1, no. 25).

sponding ΔH_f is −288 kcal/mol (no. 17). This is very close to ΔH_f for the tautomeric model with a proton at MI516(Nϵ) (no. 18) and for a positively charged $MI516^+$(NδNϵ) (no. 23). Density functional calculations for isolated flavins predict a tautomerization from the hydrogen bond to N5 to the terminal oxygen atom without activation barrier [53]. Similarly, PM3 calculations predict that such a tautomerization at the flavin in the GOX active site may lead to a more stable system when the hydrogen atom is located at the terminal oxygen instead of N5 (no. 25). For this tautomeric system with $Fl_{red}OOH_2^-$(N3O) the hydrogen bonding system is different. An intermolecular hydrogen bond with a distance of 1.85 Å exists between the oxygen atom at C4a and MI516 Nϵ after imidazole ring rotation and an intramolecular hydrogen bond C4aOOH···N5 of 1.84 Å stabilizes the flavin (Figure 8, bottom). As His^{516} is protonated at different sites in these models, a tautomerization involving an $MI516^+$(NδNϵ) might occur in the oxidative half reaction.

Influence of the protein environment and the solvent

The results of the previous section show that the catalytic function of GOX depends not only on the flavin co-enzyme but also on other residues at the active site. But a further influence of environment residues participating not directly in the chemical reaction is also an important factor for the function. For example, the heat of formation difference between the GOX substrate and product complexes (Table 1, nos. 1 and 10) is 55 kcal/mol in the protein environment, but the single point difference of the same system without the enzyme environment is only 19 kcal/mol. To analyse this effect in more detail, we removed specific residues from the PCM environment and repeated the determination of the relative ΔH_f at fixed structures of the quantum system. In general, several residues contribute to the ΔH_f difference between gas phase and PCM environment. In some cases, large contributions of a single residue exist. Almost 12 kcal/mol of the above-mentioned environmental contribution is provided by Asn^{107} located at the *si*-side of the isoalloxazine ring in the GOX structure (Figure 8), whereas the residues of helix 13 appear to be unimportant for this difference.

In Table 2 detailed differences between the gas phase and PCM heats of formation are listed. The data comparison refers to the active site quantum system without glucose and gluconolactone. In other

words, the environment effects on the catalytically active residues of GOX have been estimated for the oxidized enzyme prior to substrate approach, the reduced enzyme after product release and for those species participating in the oxidative half reaction. For the oxidized (nos. 1 and 2) and two-electron reduced enzyme (nos. 10 and 11), the most stable system is identical in the presence and absence of the environment, except for a tautomerization at MI516. A comparison with the corresponding entries of Table 1 shows that these tautomeric states are also the most stable ones in the presence of glucose or gluconolactone, respectively. For the proton transfer to MI516 the relative energy remains unchanged when the environment is removed, but the protein environment favours especially the most stable reduced enzyme state since the energy difference to the other protonation states is increased in the presence of the enzyme environment (nos. 11–16). Asn^{107} contributes approximately 9 kcal/mol to the higher stability of the negatively charged $Fl_{red}H_2^-$(N3N5) (nos. 10–13) relative to the neutral $Fl_{red}H_3$(N1N3N5) (nos. 14–15) in the PCM environment. The $\Delta\Delta H_f$ decrease of $Fl_{red}OOH_2^-$(N3O) (no. 25) relative to $Fl_{red}OOH_2^-$(N3N5) (no. 17) by the enzyme environment cannot be attributed to the presence of a single residue. The energy differences for the different protonation sites of His^{516} are particularly small. Table 1 indicates that the heats of formation are somewhat lower if His^{516} is protonated at Nδ because a hydrogen bond to the carboxamide oxygen of Gln^{329} can be formed. If the latter residue is removed from the PCM environment, a hydrogen atom at Nϵ of His^{516} leads to slightly lower heats of formation.

To estimate the influence of a solvent on the model system, we have carried out calculations of ΔG_s^0 for the quantum system at fixed geometries without the enzyme environment. The relative values $\Delta\Delta G_s^0$ in each redox state are generally smaller than the corresponding $\Delta\Delta H_f$ values in the presence of the enzyme environment. Similarly to the enzyme environment and contrary to the gas phase, the solvent favours also a hydrogen atom at MI516 Nδ relative to Nϵ in the oxidized and reduced enzyme state. $\Delta\Delta G_s^0$ for the reduced enzyme with a double protonated MI516 is much smaller than $\Delta\Delta H_f$ in the protein environment or in vacuum. As an alternative approach to estimate solvent effects semiempirically, we have taken water molecules at the active site from an MD snapshot, computed their charges with the natural atomic orbital/point charge model and added these molecules to the fixed PCM enzyme environment. With this solvent model we obtained also the same energy order for the protonation sites of MI516 predicted by the continuum model. The relative energies for the quantum system with any oxygen bond to the reduced flavin are very different in the enzyme environment compared to vacuum or continuum solvent calculations.

Discussion

We carried out computations at three different levels to derive information about the interactions of GOX with the substrate and product. First we used docking methods to derive the orientations of glucose and gluconolactone at the active site. Then force field methods were applied to find low-energy conformations for side chains and enzyme ligands. Finally, semiempirical calculations were performed to compare the energies of tautomeric states.

We decided to use the PM3 method for our model study of the mode of action of GOX, because it has been shown previously that this method is able to compute heats of formation with reasonable accuracy [47]. It can describe a series of hydrogen bonds [56, 57] and proton transfer processes [58]. PM3 gives accurate results for the heats of formation and proton affinities of imidazole and acetic acid derivatives. To our knowledge, such experimental data are not available for comparison with our FAD model. The similarity of the computed proton affinities of imidazole and methyl imidazole indicates that the truncation of alkyl side chains for the generation of model compounds is of minor influence on the relative energies. The PM3-SM3.1 solvent model has predicted relative free energies of solvation for MI516 tautomers being consistent with force field calculations with explicit water molecules at the active site.

The applied point charge model used for the enzyme environment can describe molecular multipole moments and electrostatic potentials with a high accuracy [45]. Test calculations with an enzyme environment augmented with additional residues consisting of certain secondary structure elements like helix 13 pointing towards the FAD do not lead to significant changes of the relative heats of formation. This indicates that the selected number of environment residues is sufficient. Continuum solvent model calculations, which cannot take into account simultaneously the active site environment, have been used to estimate whether or not the solvent might change the relative

Table 2. Relative heats of formation $\Delta\Delta H_f$ for the active site model[a] (in the protein PCM environment and gas phase) and relative free energies of solvation $\Delta\Delta G_s^0$

					$\Delta\Delta H_f$ (protein) (kcal/mol)	$\Delta\Delta H_f$ (gas phase) (kcal/mol)	$\Delta\Delta G_s^0$ (water) (kcal/mol)
Oxidized active site model							
1	$Fl_{ox}H$(N3)	MI559(Nϵ)	$P412^-$	MI516(Nδ)	0	0	0
2	$Fl_{ox}H$(N3)	MI559(Nϵ)	$P412^-$	MI516(Nϵ)	1	−2	1
Reduced active site model							
10	$Fl_{red}H_2^-$(N3N5)	MI559(Nδ)	PH412	MI516(Nδ)	0	0	0
11	$Fl_{red}H_2^-$(N3N5)	MI559(Nδ)	PH412	MI516(Nϵ)	3	−4	1
12	$Fl_{red}H_2^-$(N3N5)	$MI559^+$(NδNϵ)	$P412^-$	MI516(Nδ)	27	17	18
13	$Fl_{red}H_2^-$(N3N5)	$MI559^+$(NδNϵ)	$P412^-$	MI516(Nϵ)	33	16	20
14	$Fl_{red}H_3$(N1N3N5)	MI559(Nϵ)	$P412^-$	MI516(Nδ)	40	12	12
15	$Fl_{red}H_3$(N1N3N5)	MI559(Nϵ)	$P412^-$	MI516(Nϵ)	43	9	15
16	$Fl_{red}H_2^-$(N3N5)	MI559(Nϵ)	$P412^-$	$MI516^+$(NδNϵ)	41	36	14
Reduced active site model with oxygen							
17	$Fl_{red}OOH_2^-$(N3N5)	MI559(Nδ)	PH412	MI516(Nδ)	0	0	0
18	$Fl_{red}OOH_2^-$(N3N5)	MI559(Nδ)	PH412	MI516(Nϵ)	0	-10	4
19	$Fl_{red}OOH_2^-$(N3N5)	$MI559^+$(NδNϵ)	$P412^-$	MI516(Nδ)	26	11	15
20	$Fl_{red}OOH_2^-$(N3N5)	$MI559^+$(NδNϵ)	$P412^-$	MI516(Nϵ)	26	12	20
23	$Fl_{red}OOH_2^-$(N3N5)	MI559(Nϵ)	$P412^-$	$MI516^+$(NδNϵ)	−1	29	18
Reduced model with oxygen (tautomeric flavin)							
24	$Fl_{red}OOH_2^-$(N3O)	MI559(Nδ)	PH412	MI516(Nδ)	−24	−9	−6
25	$Fl_{red}OOH_2^-$(N3O)	MI559(Nδ)	PH412	MI516(Nϵ)	−57	−15	−3
26	$Fl_{red}OOH_2^-$(N3O)	MI559(Nϵ)	$P412^-$	$MI516^+$(NδNϵ)	−25	16	7
27	$Fl_{red}OOH_3$(N3N5O)	MI559(Nϵ)	$P412^-$	MI516(Nδ)	−31	−8	−6
28	$Fl_{red}OOH_3$(N3N5O)	MI559(Nϵ)	$P412^-$	MI516(Nϵ)	−25	−10	−2

[a]Rows are numbered according to Table 1.

order of different tautomeric states. It is likely that solvent effects are overestimated because the active site is located at the bottom of a deep funnel inside of the protein and the catalytic residues are only in part solvent accessible.

However, some open questions remain. PM3 predicts that a small activation energy for the proton transfer from the imidazolium ion to the oxygen of the acetate is necessary, which does not agree with our non-empirical calculations at the MP2 and B3LYP levels. To analyse the interaction between a Glu and a protonated His, ab initio calculations at a more sophisticated level might be helpful to provide a reference. Since we cannot carry out full transition state searches in the presence of harmonically constrained atoms, we cannot predict activation energies and the sequence of the transferred hydrogens. For the hydride transfer to FAD configuration interaction calculations are probably necessary. So the important questions of the rate limiting step in the reductive half reaction and potential hydrogen tunnelling [46] remain open. In the course of the oxidative half reaction, a tautomerization with a potential participation of a positively charged $MI516^+$(NδNϵ) may take place at the active site to change the initial model system (Figure 8, top) to the most stable one (Figure 8, bottom). We have made no attempts to investigate this step in detail as transition state searches with explicit water molecules filling the active site funnel after product release are probably required.

The active site of GOX is located at the bottom of a deep pocket of the enzyme, which has the shape of a funnel with a cross section of 10 Å × 10 Å at the surface and a distance between the surface and N5 of

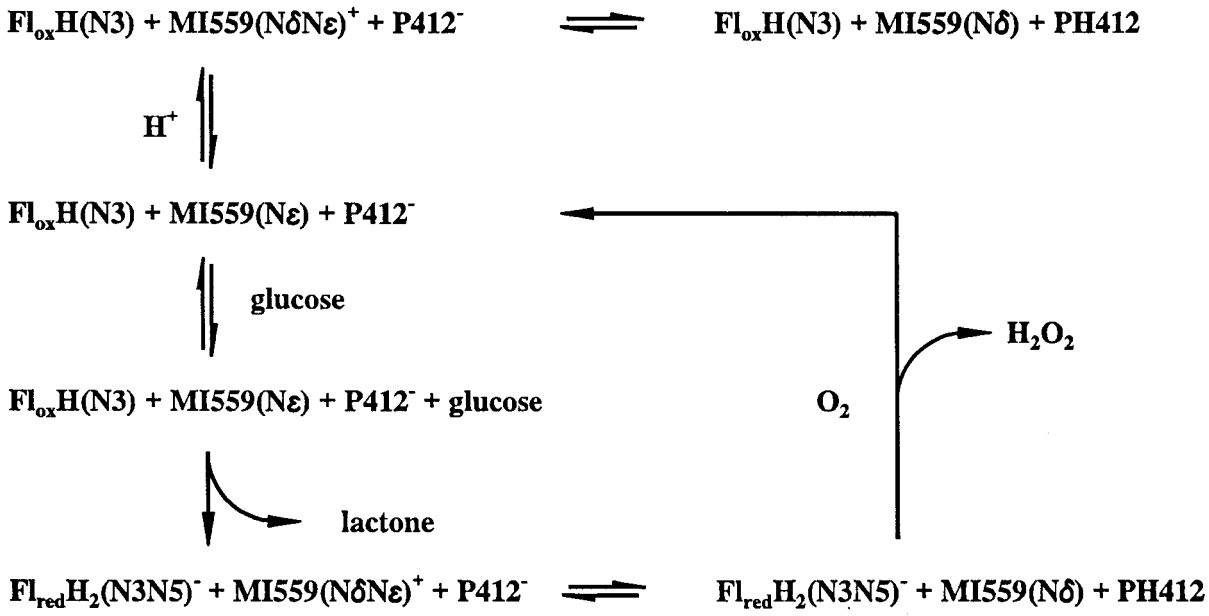

Figure 9. Proton transfer and redox reactions involving the most stable tautomers of the GOX model.

FAD in the range of 13 and 18 Å [23]. If the substrate is docked to the active site, there is only space for a water molecule on the back of His^{559} near Trp^{426} (3.9 Å from the O1 of the substrate). Continuum model calculations indicate that the most stable enzyme substrate complex remains unchanged to solvent influence.

A two-electron reduction with an N1 protonation of FAD is unlikely (see above) because the N1 is located at the opposite side of H(O1) of glucose (Figure 3). The immediate neighbours of N1 are two hydrophobic side chains (Val^{560} and Met^{561}) and two NH groups. This environment makes the addition of hydrogen improbable. Additionally, the semiempirical calculations for the model system exclude this possibility because a system with a lower heat of formation exists. The calculations indicate that the most stable product for the enzyme part of the reductive half reaction (Figure 1) is the system with a hydride ion from the glucose transferred to the N5 of Fl$_{ox}$H(N3) and a proton transferred to Nδ of MI559 with a subsequent transfer of the proton from Nϵ of MI559 to Oϵ1 of P412$^-$. The heats of formation for the reduced active site model and a potential intermediate system, which results from a transfer of the proton H(O1) from glucose to GOX, are listed in Table 1. The predicted reaction is different from the reduction of free flavins with a transfer of both hydrogen atoms to N1 and N5 of the isoalloxazine ring. This is a part of the role of the enzyme environment in catalysis. The model system with both hydrogens at N5 and N3 of Fl$_{red}$H$_2^-$(N3N5) is the most stable one. In free flavins, a two-electron reduction involves a hydrogen transfer to N1 and N5.

In principle, O4α of FAD is accessible at the active site to accept a proton. But to our knowledge, a proton at O4α has not been observed in flavins. For 10-methyl isoalloxazine the two-electron reduced tautomer with a proton at O4α is 18.1 kcal/mol less stable at the Hartree-Fock level and 8.8 kcal/mol less stable at the PM3 level [51] than the corresponding tautomer with a proton at N1. Furthermore, this species is much more energetically unfavourable in the enzyme environment.

Comparison with experiments

Manstein et al. [59] reconstituted GOX with FAD analogs and derived the absolute stereochemistry for the interaction with glucose. The experiments indicate, in correspondence with our computed enzyme substrate structures, that the substrate interacts with the *re*-face of the flavin (Figure 3). Our calculations agree well with the interpretation of the pH dependence of kinetic data [2]. The model depicted in Figure 9 is an extension of their proposal based on kinetic investigations, which did not contain the detailed interaction of glucose with additional residues of the active site since the 3D structure was unknown. They pointed out

that a carboxylate group must be involved in the substrate binding of the enzyme and that the protonated oxidized enzyme has little or no binding affinity for glucose. In fact our modelled substrate complex predicts a hydrogen bridge between the Oδ2 of Asp^{424} and H(O4) of glucose at the semiempirical level. Furthermore, the carboxyl group of Glu^{412} can also be protonated, which destroys the charge relay system acting on H(O1) of glucose. The breaking of the hydrogen bond between H(Nϵ) of His^{559} and Glu^{412} may also lead to a different orientation of the His side chain so that Nδ can no longer participate in substrate binding.

The reductive half reaction leads to gluconolactone and the reduced system of the active site (Figure 9). In this system, a hydride is transferred to N5 of the FAD and a proton to Nδ of MI559, which forms a catalytic dyad with $P412^-$. No indications for a radical mechanism have been observed in EPR experiments [2]. Our semiempirical model calculations show that the following protonation of $P412^-$ leads to the lowest heat of formation (Table 1, no. 10).

Even though the GOX structure was not known at that time, Weibel and Bright proposed, on the basis of kinetic data, that the hydrogen atom at N3 forms a hydrogen bond with the enzyme and the breaking of this bond may cause changes of the planarity of the isoalloxazine nucleus, which should influence the reactivity. Such a hydrogen bond between the N3 donor and the Thr^{110} backbone oxygen acceptor atom indeed exists in the experimental protein structure [23]. Unlike planar free oxidized flavins, the co-enzyme has a non-planar butterfly-type structure in the protein with a fold angle of 16.4° along the N5-N10 axis in the oxidized state of the GOX. The FAD is fixed by hydrogen bonds and sterical constraints which probably activate FAD. Therefore, one may think that the removal of the hydrogen bond may lead to a deformation of the fold angle and thus may influence the reactivity, because the isoalloxazine ring is already folded in an angle, which is energetically favourable in the reduced state. The energy minimum of the anionic two-electron reduced isoalloxazine corresponds to a fold angle of 14.7° [53]. But the energy difference between the planar and folded structure is very small in the two-electron reduced state. Therefore, the fold can only affect the activation energy of the flavin redox reaction.

Our prediction is also in agreement with a ^{15}N NMR study [60]. The analysis of the spectra shows that the reduced flavin of GOX is negatively charged at pH 5.6 with hydrogen at N3 and N5. N1 of the reduced FAD does not contain a hydrogen. These experimental results are indeed part of our prediction.

Related enzymes

The proposed mechanism is also relevant for the homologous enzyme family termed GMC oxidoreductases, which include glucose dehydrogenase, choline dehydrogenase, cholesterol oxidase, alcohol oxidase and GOX. According to the sequence alignment carried out by Cavener [4] in all four enzymes an Asn corresponding to Asn^{107} in GOX (Figure 8) is conserved. Furthermore, in cholesterol oxidase [61] the relative orientation of an Asn to the isoalloxazine ring is much the same as Asn^{107} in the GOX structure. It would appear, then, that the interaction between Asn and the flavin is a general feature of GMC oxidoreductases. According to our calculations, this residue contributes to the energy difference between the GOX complexes with the substrate and product. It is also important to prevent a proton transfer to the flavin N1 atom.

A superposition of the GOX and cholesterol oxidase active site shows a further common structural feature between both enzymes. The coupling between His^{516} and Gln^{327} in GOX (Figure 8) exists between His^{447} and Asn^{323} in cholesterol oxidase having a similar relative orientation. The His of this pair is conserved in all GMC oxidoreductases. The main difference between both GOX and cholesterol oxidase is the presence of the His^{559}, which has no counterpart in cholesterol oxidase. Li et al. [61] assumed that the mechanism of the proton abstraction from the hydroxy group of the substrate is the same for both enzymes, and this line of thinking led them to the conclusion that H(O1) of glucose must be transferred to His^{516} because a His corresponding to His^{559} is missing in cholesterol oxidase. Our view of this is that the protons of the hydroxy groups of different substrates may be abstracted by different mechanisms in different enzymes. The calculations indicate that His^{516} is of central importance for GOX even though a proton transfer to His^{559} leads to more stable products. It seems more likely that the conserved His might be involved in the common step of the enzymatic reactions, which is the oxidative half reaction of the FAD. Furthermore, His^{516} can stabilize an oxyanion with a Cϵ-H$\cdots$O(1) hydrogen bond. Such non-standard hydrogen bonds with a carbon donor atom have been found recently in a series of biopolymers [62,63], but

their individual energetical contribution is probably low [64]. A proton transfer to His^{516} might be possible at a lower pH if His^{559} is protonated during the complete catalytic cycle. But the energy difference between the enzyme substrate and product complexes is smaller in this case.

In the X-ray structure of cholesterol oxidase with dehydroandrosterone a single water molecule is at the active site, which is believed to mediate proton transfer [61]. We have placed a water molecule at the corresponding position in the GOX enzyme substrate complex and optimized the structure. However, this position close to His^{516} does not correspond to a local energy minimum. This might indicate that a water-mediated proton transfer does not take place in the enzymatic reaction of GOX.

Conclusions

The combination of classical and quantum mechanical methods is a powerful tool for the study of enzymatic catalysis. We have determined substrate binding residues presented a catalytic mechanism for GOX, which is consistent with experimental data. The calculations show that only the hydride ion is transferred to the FAD co-enzyme. His^{516} plays an important role in the reductive and oxidative half reaction. In addition to the chemically active residues, the enzyme environment is important for the stabilization of the products of the reductive half reaction.

Acknowledgements

We thank H.J. Hecht for providing the X-ray structure of glucose oxidase and H.M. Kalisz for stimulating discussions. A portion of this work was supported by a European Union Access to Large Scales Facilities grant (ERBCHGECT940062) to EMBL.

References

1. Combs, B.S., Carper, W.R. and Stewart, J.J.P., J. Mol. Struct. (THEOCHEM), 258 (1992) 235.
2. Weibel, M.K. and Bright, H.J., J. Biol. Chem., 246 (1971) 2734.
3. Müller, F., In Müller, F. (Ed.) Chemistry and Biochemistry of Flavoenzymes, Vol. 1, CRC Press, Boca Raton, FL, 1991, pp. 1–71.
4. Cavener, D.R., J. Mol. Biol., 223 (1992) 811.
5. Ritter von Onciul, A. and Clark, T., J. Comput. Chem., 14 (1993) 392.
6. Ciarkowski, J. and Oldziej, S., Eur. Biophys. J., 22 (1993) 207.
7. Andrés, J., Safort, V.S., Martins, J.B.L., Beltrán, A. and Moliner, V., J. Mol. Struct. (THEOCHEM), 330 (1995) 411.
8. Venanzi, T.J., Bryant, B.P. and Venanzi, C.A., J. Comput.-Aided Mol. Design, 9 (1995) 439.
9. Chang, C.-C. and Huang, P.C., Protein Eng., 9 (1996) 1165.
10. Silva, A.M., Cachau, R.E., Sham, H.L. and Erickson, J.W., J. Mol. Biol., 255 (1996) 321.
11. Stavrev, K.K. and Zerner, M.C., Chem. Eur. J., 2 (1996) 83.
12. Cunningham, M.A., Ho, L.L., Nguyen, D.T., Gillian, R.E. and Bash, A., Biochemistry, 36 (1997) 4800.
13. Peräkylä, M. and Pakkanen, T.A., J. Am. Chem. Soc., 115 (1993) 10958.
14. Beveridge, A.J. and Ollis, D.L., Protein Eng., 8 (1995) 135.
15. Damborský, J., Kutý, M., Němec, M. and Koča, J., J. Chem. Inf. Comput. Sci., 37 (1997) 562.
16. Hu, H., Liu, H. and Shi, Y., Proteins, 27 (1997) 545.
17. Mulholland, A.J. and Richards, W.G., Proteins, 27 (1997) 9.
18. Wladkowski, B.D., Krauss, M. and Stevens, W.J., J. Am. Chem. Soc., 117 (1995) 10357.
19. Alagona, G., Ghio, C. and Kollman, P.A., J. Mol. Struct. (THEOCHEM), 371 (1996) 287.
20. Lee, H., Darden, T.A. and Pedersen, L.G., J. Am. Chem. Soc., 118 (1996) 3946.
21. Garmer, D.R., J. Phys. Chem., B101 (1997) 2945.
22. Mulholland, A.J., Grant, G.H. and Richards, W.G., Protein Eng., 6 (1993) 133.
23. Hecht, H.J., Kalisz, H.M., Hendle, J., Schmid, R.D. and Schomburg, D., J. Mol. Biol., 229 (1993) 153.
24. Meyer, M., Wilson, P. and Schomburg, D., J. Mol. Biol., 264 (1996) 199.
25. Chu, S.S.C. and Jeffrey, G.A, Acta Crystallogr., 24 (1968) 830.
26. Schomburg, D. and Reichelt, J., J. Mol. Graph., 6 (1988) 161.
27. Pearlman, D.A., Case, D.A., Caldwell, J.C., Seibel, G.L., Singh, U.C., Weiner, P. and Kollman, P.A, AMBER 4.0, University of California, San Francisco, CA, U.S.A., 1991.
28. Cornell, W.D., Cieplak, P., Bayly, C.I., Gould, I.R., Merz, K.M., Ferguson, D.M., Spellmeyer, D.C., Fox, T., Caldwell, J.W. and Kollman, P.A., J. Am. Chem. Soc., 117 (1995) 5179.
29. Woods, R.J., Dwek, R.A. and Fraser-Reid, B., J. Phys. Chem., 99 (1995) 3832.
30. Voet, J.G., Coe, J., Epstein, J., Matossian, V. and Shipley, T., Biochemistry, 20 (1981) 7182.
31. Jorgensen, W.L., Chandrasekhar, J., Madura, J.D., Imey, R. and Klein, M., J. Chem. Phys., 79 (1983) 926.
32. Ryckaert, J.P., Cicotti, G. and Berendsen, H.J.C., J. Comput. Phys., 23 (1977) 327.
33. Cox, S.R. and Williams, D.E., J. Comput. Chem., 2 (1981) 304.
34. Singh, U.C. and Kollman, P.A., J. Comput. Chem., 5 (1984) 129.
35. Lee, C., Yang, W. and Parr, R.G., Phys. Rev., B37 (1988) 785.
36. Becke, A.D., J. Chem. Phys., 98 (1993) 5648.
37. Hehre, W.J., Ditchfield, R. and Pople, J.A., J. Chem. Phys., 56 (1972) 2257.
38. Peräkyla, M. and Pakkanen, T.A., Proteins, 21 (1995) 22.
39. Frisch, M.J., Trucks, G.W., Schlegel, H.B., Gill, P.M.W., Johnson, B.G., Robb, M.A., Cheeseman, J.R., Keith, T., Petersson, G.A., Montgomery, J.A., Raghavachari, K., Al-Laham, M.A., Zakrzewski, V.G., Ortiz, J.V., Foresman, J.B., Cioslowski, J., Stefanov, B.B., Nanayakkara, A., Challa-

combe, M., Peng, C.Y., Ayala, P.Y., Chen, W., Wong, M.W., Andres, J.L., Replogle, E.S., Gomperts, R., Martin, R.L., Fox, D.J., Binkley, J.S., Defrees, D.J., Baker, J., Stewart, J.P., Head-Gordon, M., Gonzalez, C. and Pople J.A., GAUSSIAN 94, Revision B.3, Gaussian Inc., Pittsburgh, PA, U.S.A., 1995.
40. Schmidt, M.W., Baldridge, K.K., Boatz, J.A., Elbert, T.S., Gordon, M.S., Jensen, J.H., Koseki, S., Matsunaga, N., Nguyen, K.A., Su, S., Windus, T.L., Dupuis, M. and Montgomery, J., J. Comput. Chem., 14 (1993) 1347.
41. Stewart, J.J.P., J. Comput. Chem., 10 (1989) 209.
42. Vamp 6.1, Oxford Molecular Ltd., Magdalen Centre, Oxford Science Park, Sandford-on-Thames, Oxford OX4 4GA, U.K.
43. Hawkins, G.D., Lynch, G.C., Giessen, D.J., Rossi, I., Storer, J.W., Liotard, D.A., Cramer, C.J. and Truhlar, D.G., AMSOL 5.4 Quantum Chemistry Exchange Program 606, based in part on AMPAC 2.1, Liotard, D.A., Healy, E.F., Ruiz, J.M. and Dewar, M.J.S.
44. Liotard, D.A., Hawkins, G.D., Lynch, G.C., Truhlar, D.G. and Cramer, C.J., J. Comput. Chem., 16 (1995) 422.
45. Beck, B., Rauhut, G. and Clark, T., J. Comput. Chem., 15 (1994) 1064.
46. Kohen, A., Jonsson, T. and Klinman, J.P., Biochemistry, 36 (1997) 2603.
47. Stewart, J.J.P., J. Comput.-Aided Mol. Design, 4 (1990) 1.
48. Meyer, M., J. Mol. Struct. (THEOCHEM), 304 (1994) 45.
49. NIST Chemistry Web Book, NIST Standard Reference Database Number 69, August1997 Release (http://webbook.nist.gov/chemistry). Proton affinity data compiled and evaluated by E.D. Hunter and S.G. Lias.
50. Schröder, S., Daggett, V. and Kollman, P.A., J. Am. Chem. Soc., 113 (1991) 8922.
51. Meyer, M., Hartwig, H. and Schomburg, D., J. Mol. Struct. (THEOCHEM), 364 (1996) 139.
52. Zheng, Y.-J. and Ornstein, R.L., J. Am. Chem. Soc., 118 (1996) 9402.
53. Meyer, M., J. Mol. Struct. (THEOCHEM), 417 (1997) 163.
54. Wouters, J., Durant, F., Champagne, B. and André, J.-M., Int. J. Quantum Chem., 64 (1997) 721.
55. Massey, V., J. Biol. Chem., 269 (1994) 22459.
56. Jurema, M.W. and Shields, G.C., J. Comput. Chem., 14 (1992) 89.
57. Lively, T.N., Jurema, M.W. and Shields, G.C., Int. J. Quantum Chem., 21 (1994) 95.
58. Kallies, B. and Mitzner, R., J. Mol. Model., 1 (1995) 68.
59. Manstein, D.J., Pai, F., Schopfer, L.M. and Massey, V., Biochemistry, 25 (1986) 6807.
60. Sanner, C., Macheroux, P., Rüterjans, H., Müller, F. and Bacher, A., Eur. J. Biochem., 196 (1991) 663.
61. Li, J., Vrielink, A., Brick, P. and Blow, D.M., Biochemistry, 32 (1993) 11507.
62. Derewenda, Z.S., Derewenda, U. and Kobos, P.M., J. Mol. Biol., 241 (1994) 83.
63. Wahl, M.C. and Sundaralingam, M., Trends Biochem. Sci., 22 (1997) 97.
64. Ornstein, R.L. and Zheng, Y.L., J. Biomol. Struct. Dyn., 14 (1997) 657.
65. Kraulis, P., J. Appl. Crystallogr., 24 (1991) 946.